Colloid Polym Sci (2009) 287:471–479
DOI 10.1007/s00396-009-1995-2

ORIGINAL CONTRIBUTION

Synthesis of crosslinked polymer nanoparticles suitable for the formation of nanolayer organic films

Andrea Uveges · John F. Hartmann · Lajos Daroczi · Janos Borbely

Received: 31 July 2008 / Revised: 26 November 2008 / Accepted: 28 December 2008 / Published online: 20 January 2009

Abstract Free radical crosslinking copolymerization of styrene and ethylene glycol dimethacrylate (n_{ST}/n_{EGDM} in feed=5/5) has been investigated in toluene. Variation of the reaction conditions allows the formation of macromolecules with low molecular weight (21.6 kDa and 12 nm in diameter), perfectly soluble branched particles in the early stage of the polymerization. Elongation of the reaction time leads to the formation of soluble/swelling microgels with medium molecular weight (156 kDa and 41–120 nm) and, finally, swelling/particularly soluble colloidal polymer particles with very high molecular weight (3.6 MDa and 59–324 nm). Conversion, molecular weight [by gel permeation chromatography (GPC)], ratio of pendant vinyl groups [by nuclear magnetic resonance (NMR)], size of nanoparticles in swollen [by dynamic light scattering (DLS)] and dried state [by transmission electron microscopy (TEM)], morphology [by scanning electron microscopy (SEM)], and nanolayer film formation (by SEM) were measured. The role of reaction conditions in producing different polymer structures and morphologies was demonstrated.

Keywords Free radical polymerization · Nanoparticles · Nanolayer film formation

A. Uveges · J. Borbely
Department of Colloid and Environmental Chemistry,
University of Debrecen,
4010 Debrecen, Hungary

L. Daroczi
Department of Solid State Physics, University of Debrecen,
4010 Debrecen, Hungary

J. F. Hartmann
ElizaNor Polymer LLC,
1 Woodmeadow Lane,
Princeton Junction, NJ 88550, USA

J. Borbely (✉)
BBS Nanotechnology Ltd,
P.O. Box 12, 4225 Debrecen 16, Hungary
e-mail: j.borbely50@gmail.com

Introduction

A great attention has been paid to the syntheses of hyperbranched and star-shaped polymers. These materials are known for their unique structures and exhibit properties such as globular shape, high solubility, low solution viscosity, and no crystallization [1–6].

Through their special properties, these polymers of unique characteristics can be widely used in many industrial applications, such as drug delivery [7], membrane formation [8], as organofiller in dental materials [9], and as adhesives in paints and coatings [10].

It is well known that free radical copolymerization of monovinyl monomers with a small amount of divinyl monomers usually leads to gelation [11]. Soluble branched copolymer and star-shaped structures with crosslinked microgel cores have been synthesized by a number of polymerization techniques, including cationic [12, 13], anionic [14], nitroxide-mediated radical polymerization [15], atom transfer radical polymerization [16–19], and reversible addition fragmentation chain transfer radical polymerization [20].

In a series of recent papers, Sherrington et al. reported a facile ‘Stratchlyde’ route to soluble branched copolymers [21–25]. Those materials were synthesized by free radical copolymerization using a monovinyl and a divinyl monomer, typically methyl methacrylate and ethylene glycol dimethacrylate (EGDM) and a thiol as chain transfer agent.

In the presence of the chain transfer agent, the molecular weight of the primary chains is substantially reduced, and gelation can be suppressed, even at high conversion [21–25]. Armes et al. [26–29] and Wang and Zhu [30, 31] have recently extended this "Strathclyde" approach to branched copolymers to include several types of (pseudo-)living polymerizations.

Sato et al. have performed the polymerization of several divinyl monomers (e.g., divinyl adipate, EGDM, and divinylbenzene) as effective crosslinker with dimethyl 2,2′-azobisisobutyrate as initiator in homogenous solution using of large amount of initiator as a strategy to avoid crosslinking. The initiator-fragment incorporation radical polymerization resulted in the production of soluble hyperbranched polymer nanoparticles [32–34].

Qiao et al. have described the synthesis of star-like polymers by conventional free radical polymerization by exploiting differences of the reactivity ratios of monomer and crosslinker. Star-like methyl acrylate/EGDM microgels were prepared by one-pot free radical polymerization applying of small amount of crosslinker [35]. Applying this latest mentioned free radical polymerization technique, several problems can be eliminated, which otherwise occur in case of the abovementioned polymerization techniques; such problems can be, among other problems, limited choice of monomers and solvents, very strict reaction conditions, high costs, the need to remove metal catalysts, etc.

Recently, it has been revealed that in homogeneous solution, it is possible to synthesize soluble branched copolymers by free radical polymerization even by applying the crosslinking monomer in large amounts. A conversion rate of 65% was achieved (without macrogelation detected) with polymerization of monomers in 1:1 molar ratio [styrene (ST)/EGDM] [36].

In this paper, the successful synthesis of soluble copolymers of ST with large amounts of EGDM via free radical polymerization is reported. The aim was to synthesize soluble/swelling reactive polymer nanoparticles without gelation at a conversion rate nearly 100%. Special emphasis was placed on size and morphology of polymers with different molecular weight, which allow a detection of polymerization subprocesses occurring during free radical polymerization in solution.

Experimental section

Materials

Monomers applied were ST and EGDM (Aldrich); the chemical structures of these materials are shown in Fig. 1. The stabilizers of the monomers, namely, 4-*tert* butylcatechol for ST and hydroquinone monomethyl ether for EGDM were removed by extraction with 10% NaOH solution followed by extraction with distilled water. Then, the ST was distilled at low pressure, and EGDM was purified via column chromatography over Al_2O_3. The initiator 2,2-azobis (isobutyronitrile) (AIBN) obtained from Fluca was purified by recrystallization from methanol (MEOH). Monomers and initiator were stored below 4 °C before use. Toluene as solvent was used after distillation.

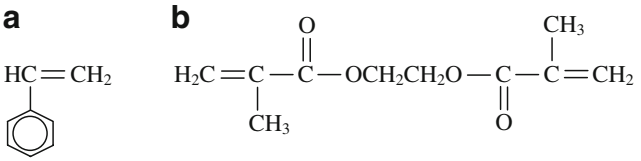

Fig. 1 Chemical structures of **a** styrene (ST) and **b** ethylene glycol dimethacrylate (EGDM) monomers

Preparation of ST-EGDM copolymeric nanoparticles

In a typical copolymerization procedure, ST, EGDM, and AIBN were dissolved in toluene under slow stream of nitrogen at room temperature for 30 min than the homogeneous solution was heated at 60 °C. The total concentration of the monomers was 0.556 and 0.278 mol/dm^3, respectively. The resulting copolymer samples were isolated by pouring the polymerization mixtures into large excess chilled methyl alcohol. Purification was done twice by dissolving in toluene and then precipitated by methanol. Parameters of synthesis procedures are summarized in Table 1.

Table 1 Free radical copolymerization of styrene (ST) and ethylene glycol dimethacrylate (EGDM) in toluene under variation of the reaction conditions

n_{ST}/n_{EGDM} in feed	[mon][a] (mol/dm^3)	AIBN[b] (mol %)	Reaction time (min)
1/1	0.278	5	120, 150, 180, 317, 597, 1310
	0.278	10	120, 240, 360, 480, 660, 1020, 1490
	0.278	20	120, 240, 360, 480, 660, 900, 1140, 1320, 1490
	0.556	5	30, 60, 120, 180, 240
	0.556	10	30, 60, 90, 120, 150, 180
	0.556	20	30, 60, 90, 120, 150, 180

Solvent=toluene, T=60 °C
[a] Concentration of the total monomers
[b] Amount of AIBN based on the total amount (mol) of monomers

Measurements

Nuclear magnetic resonance spectroscopy ^{1}H nuclear magnetic resonance (NMR) spectra were recorded on a Bruker 200 SY NMR spectrometer at 200 MHz, and deuterated chloroform ($CDCl_3$) was used as a solvent. In the case of the spectra of the samples dissolved in $CDCl_3$, the integral value of the residual $CHCl_3$ peak at 7.26 ppm had to be subtracted from that of the wide peak of the ST unit of the copolymer.

Gel permeation chromatography Gel permeation chromatography (GPC) measurements were carried out using a Waters chromatograph equipped with four gel columns (7.8×300 mm, Styragel HR3, HR4, HR5, and HR6), a Waters 600 HPLC pump, and with Waters 490E UV and Waters 410 refractive index detectors. Calibration was carried out using polystyrene standards with peak molecular weights (M_p) in the range 581–7,520,000 g/mol in solution of tetrahydrofuran (c=0.5% m/m). The determined molecular weights are not absolute values but "polystyrene equivalents."

Dynamic light scattering Dynamic light scattering (DLS) measurements were carried out by a Brookhaven Laser Light Scattering Research System at λ=532 nm. In the application of DLS for particle sizing and size distribution, the autocorrelation functions were at 90° angle and at 25 °C. The macromolecular concentration in a toluene solution was 0.01–0.4 mg/cm^3.

Transmission electron microscopy A Hitachi S-4300 transmission electron microscope was used to characterize the size and morphology of the dried ST-EGDM copolymer nanoparticles. Samples were prepared as follows: Polymer was dissolved in chloroform (0.5 mg/ml); then, some methanol was introduced drop by drop (until opalescence appeared). The sample was then dropped on carbon-coated copper grid. Methanol was used in the course of transmission electron microscopy (TEM) sample drying in order to suppress aggregation of polymer nanoparticles. In addition, some drops of sodium dodecyl sulfate (SDS) tenside solution with 0.08 mol/dm^3 concentration were added to the polymer solution sample with the lowest molecular weight. It was dried at room temperature and then examined by TEM without any further modification or coating. Mean diameter and the size distribution were obtained from measured particles visualized by TEM images.

Scanning electron microscopy The morphological characterization of the copolymer particles was carried out with a Hitachi 3000N scanning electron microscope. Drops of copolymer solution (10:1 mixture of chloroform and methanol) were placed on a carbon film coated on a copper grid and then were dried at room temperature. According to the preparation of TEM samples, some drops of SDS solution at a concentration of 0.08 mol/dm^3 were added to the lowest molecular weight polymer solution before placing on the copper grid. Pure chloroform solution of polymers was dropped on the carbon-coated copper grid to investigate the nanolayer film formation. Observation was done at an accelerating voltage of 30 kV.

Result and discussion

Conversion

Figure 2 shows the conversion values as a function of the polymerization time for all of the polymerization conditions studied (monomer ratio ST/EGDM=1/1 in the feed; total amount of monomers, 0.556 and 0.278 mol/dm^3; initiator concentration, 5, 10, and 20 mol%). The conversion was monitored up to the gelation point. At a monomer concentration of 0.556 mol/dm^3, the gelation time decreased with the increase in the concentration of the initiator. However, no macrogelation was observed at 0.278 mol/dm^3 monomer concentration. The comparison of these plots attributed to various reaction conditions as mentioned above shows different relative growth rates depending on the reaction environment. In all cases, the curves intersect the y-axis at the zero conversion, which

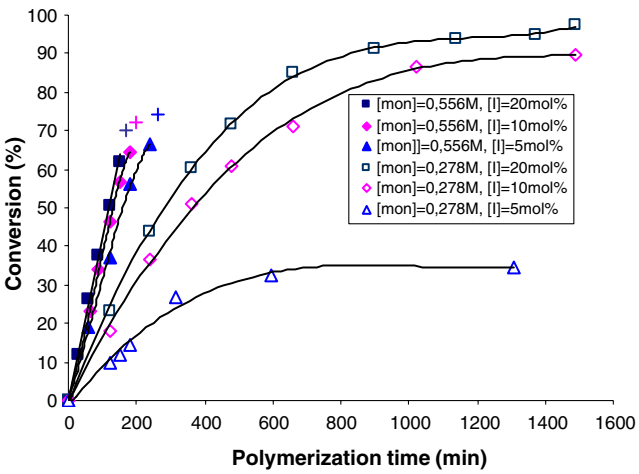

Fig. 2 Conversion values of the copolymerization of styrene (ST) and ethylene glycol dimethacrylate (EGDM) using different reaction conditions (solvent, toluene; initiator, AIBN; amount of AIBN relative to total monomers, *square* 20 mol%; *diamond* 10 mol%; *triangle* 5 mol%. *Closed symbols* represent 0.556 M concentration of the total monomers, while *open symbols* represent 0.278 M. The gelation point is indicated by *plus symbol*

confirmed that inhibition has not taken place. Conversion at the lowest polymerization time increases linearly up to a critical reaction time, after which the growth rate declines and eventually ceases. These results show that the system of 0.556 mol/dm^3 reacts more rapidly than that of 0.278 mol/dm^3 independently on the applied AIBN concentration. Furthermore, it was found that the more AIBN was applied, the faster the polymerization reaction took place.

Experiments showed that the polymerization process is very slow at low monomer concentration (0.278 mol/dm^3) and low initiator concentration (5%); the maximum conversion gained was 35%, which can be achieved by reaction time of 700 min. However, low monomer concentration and high initiator concentration (20 mol%) together result in a very high conversion (almost 100%).

The highest possible conversion was 66% (based on the total weight of monomers) at 0.556 mol/dm^3 monomer concentration; however, nearly 100% conversion was observed at 0.278 mol/dm^3 monomer concentration at 20 mol% AIBN without gelation.

Molecular weight determined by GPC

Figure 3 represents the systems of 0.278 and 0.556 mol/dm^3 concentrations of the total monomers at 5, 10, and 20 mol% AIBN concentration and shows that the molecular weight (M_w) has an exponential increase with reaction time. It can be seen that, by using the same reaction time, much higher molecular weight can be obtained at monomer concentration of 0.556 mol/dm^3 than at 0.278 mol/dm^3. The molecular weight distribution of polymer sample synthesized at nearly 100% conversion is extremely large and has not been indicated in Fig. 3; it is shown in a separate GPC chromatogram (see Fig. 4).

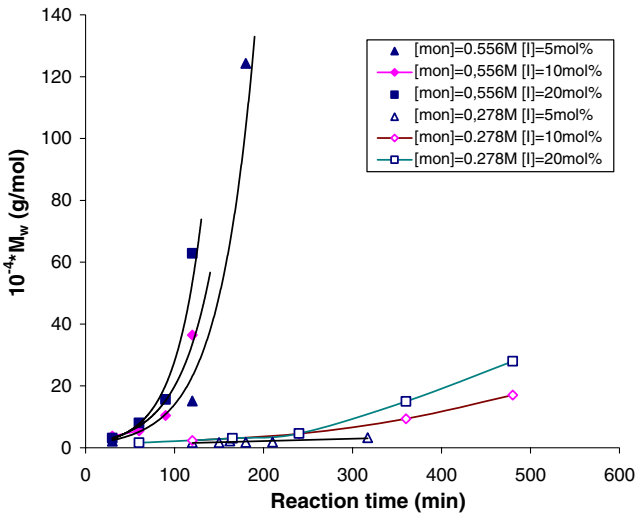

Fig. 3 M_w–reaction time curves for ST-EGDM copolymers (ST/EGDM=1/1). *Closed symbols* represent 0.556 mol/dm^3 concentration of the total monomers, while open symbols represent 0.278 mol/dm^3

Analysis of copolymer samples of low, medium, and high molecular weights

The analysis of the large number of primer data suggested that a thorough study and comparison of results of three samples can give a simplified yet comprehensive view on the processes taking place in the course of non-linear radical polymerization.

Consequently, samples with low, medium, and high molecular weights were in the focus of the analyses. Based on NMR measurements of the analyzed polymer samples, the amounts of unreacted pendant vinyl groups were calculated as described earlier [36]. The size of polymer nanoparticles in swollen (DLS) and undissolved status [TEM, scanning electron microscopy (SEM)], polymer morphology, and film-formation abilities (SEM) were analyzed. Table 2 gives an overview of reaction conditions of the selected polymers with low, medium, and high molecular weights, which are hereunder referred to as samples 1, 2, and 3, respectively.

Molecular weight and polydispersity

Figure 4 and Table 3 provide the results of GPC analysis of the three selected polymer samples. The shapes of chromatograms of samples with low, medium, and high molecular weights indicate a typical difference. The GPC trace of sample 1 is symmetric, spreads widely and distorted asymmetrically for sample 2, whereas sample 3 shows multimodal distribution with several peaks. Note that the GPC curves tend to drift to lower elution times as molecular weight increases, just as the literature indicates. The variance in the behaviors of the curves and drift along with elution time clearly reflects the vast differences in polydispersity and molecular weights of the samples.

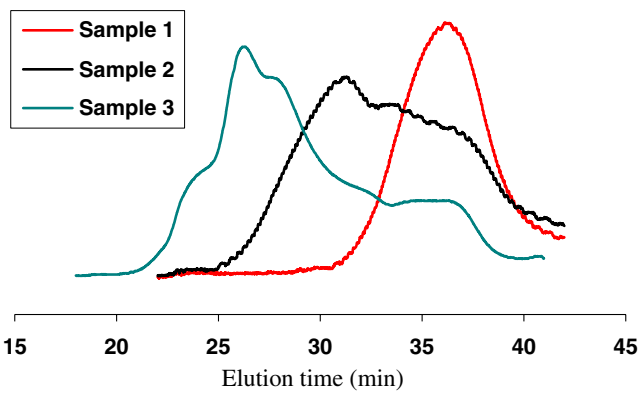

Fig. 4 GPC traces of the low (sample 1), medium (sample 2), and high molecular weight (sample 3) polymers

Table 2 Reaction conditions of the selected low, medium, and high molecular weight copolymer samples

Sign of polymers	[mon][a] (mol/dm^3)	AIBN[b] (mol %)	Reaction time (t_r)
Sample 1	0.556	5	30 min
Sample 2	0.556	20	90 min
Sample 3	0.278	20	22 h

[a] Concentration of the total monomers
[b] Amount of AIBN based on the total amount (mol) of monomers

Table 3 summarizes the conversion and the average molecular weight (M_w), the peak molecular weight ($M_{w,p}$), and polydispersity (PDI) after evaluating GPC measurements. It is indicated that polydispersity increases with higher molecular weight. In case of sample 3, a very high polydispersity, about PDI=49, was observed at average molecular weight of approximately 3.6 million Daltons. This very high PDI can be demonstrated well with the large difference in molecular weights corresponding to two adjacent peaks in the chromatogram. The molecular weight corresponding to the maximum in the distribution curve is about 1.3 million Daltons, whereas as much as 13.2 million Daltons can be assigned to the 'shoulder' at the lowest elution time.

Calculating a single value of PDI is not valid for a multimodal system; therefore, it should be noted that the PDI data shown in Table 3 has only qualitative importance for the multimodal GPC curve of the sample 3.

Reactivity of the copolymers

On the basis of ^{1}H NMR spectrum of polymeric nanoparticles, the ratio of pendant vinyl groups was determined. Percentage amount of pendant vinyl groups were calculated in line with the method presented in previous publications [36, 37].

Unreacted pendant double-bond contents of samples 1, 2, and 3 are 54.3, 47.5, and 16.3%, respectively.

Table 3 Summary of final conversions, molecular weights and polydispersities (PDI) of samples 1, 2, and 3 of ST-EGDM copolymers

Sign of polymers	Sample 1	Sample 2	Sample 3
M_w by GPC[a] (Da)	21,600	156,000	3,628,400
$M_{w,p}$ by GPC[a] (Da)	17,000	120,000	1,393,000
PDI by GPC	1.5	3.3	49.0
GPC curve shape	mo	sh	mu
Conversion (%)	9.5	37.6	94.5

mo monomodal, *sh* shoulder, *mu* multimodal
[a] $M_{w,p}$ was determined using polystyrene calibration; results are not absolute values, but "polystyrene equivalents" (*p* peak)

Particle size in swollen state: laser light scattering studies

Figure 5 shows the DLS measurements performed on ST/EGDM copolymer samples, which were of various molecular weights and dissolved/swollen in toluene. The size distributions were calculated by non-negatively constrained least squares (NNLS).

Average hydrodynamic diameters ($\langle d \rangle_{int}$) of samples 1, 2, and 3 as per intensity were 12±1, 58±3, and 152±5 nm, respectively, and the distribution curves of the samples differed highly. The distribution curve of sample 1 is monomodal and shows narrow distribution in size (11.3–

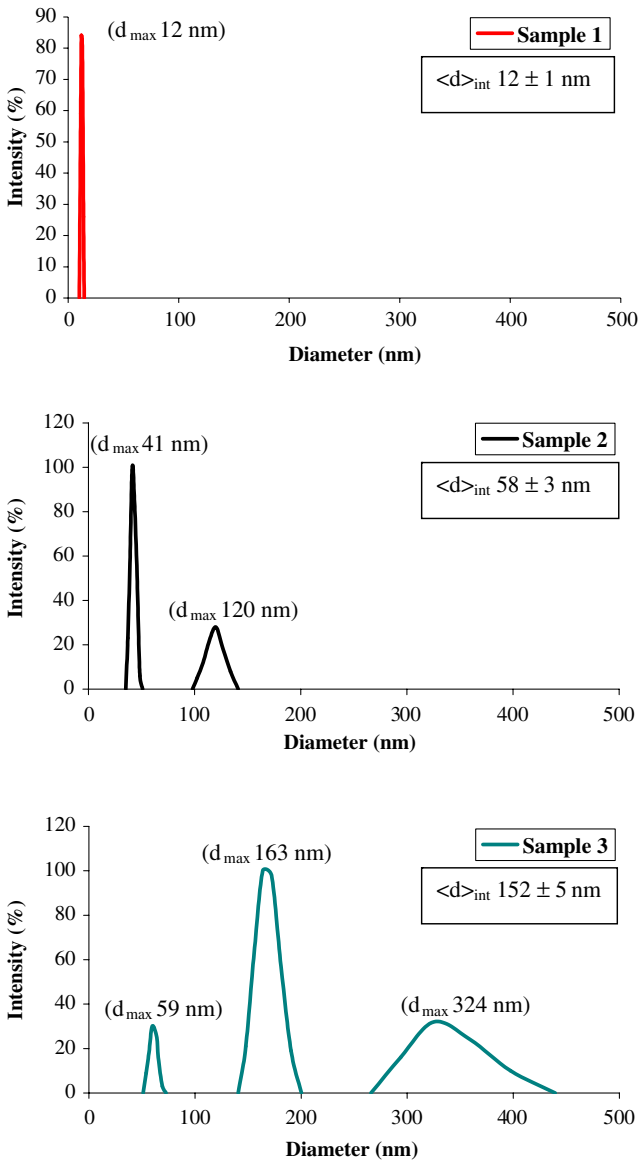

Fig. 5 Intensity–size distributions obtained by DLS at Θ=90°, λ=532 nm, calculated by NNLS (sample 1: ST/EGDM=1/1, [mon]=0.556 mol/dm^3, AIBN=5 mol%, t_r=30 min; sample 2: ST/EGDM=1/1, [mon]=0.556 mol/dm^3, AIBN=20 mol%, t_r=90 min; sample 3: ST/EGDM=1/1, [mon]=0.278 mol/dm^3, AIBN=20 mol%, t_r=22 h)

14.4 nm), and the hydrodynamic diameter corresponding to the maximum intensity is 12 nm, which equals to the average hydrodynamic diameter as per intensity. The distribution curve of sample 2 is bimodal, and the hydrodynamic diameters of the detected particles were in the ranges of 37–51 and 102–134 nm. Hydrodynamic diameters of 41 and 120 nm belong to the maximum intensity values of the two peaks in the distribution curve. The fact that the hydrodynamic diameter of polymer nanoparticles were between 54 and 440 nm nicely reflects the highly polydisperse characteristics of sample 3. The distribution curve shows fairly polydisperse status indicated by several maximum plots (59, 163, and 324 nm). In sum, we can state that the average values increase and the distribution curves shift toward the large molecular size region. The results obtained with light scattering correlate with the results of GPC measurements.

Particle size in dried form measured by TEM

Figure 6 illustrates the transmission electron micrographs of polymers with low (sample 1), medium (sample 2), and high (sample 3) molecular weights and the size distributions, respectively. Particle size distribution in sample 1 is monomodal and shows a wide size range, the polymer sample consists of particles between 50 and 353 nm, and the diameter of the most frequent copolymer particles was 180 nm. At the same time, the image taken of the sample shows a decreased contrast and particle contour is rather blurred, which indicates that polymeric nanoparticles have flattened shape in the sample. Such flattened shape evolves only if the produced particles have low crosslinking density. The unreacted pendant vinyl group content calculated on the basis of NMR spectrum is 54.3%, which means that less than 50% of double bonds on primarily

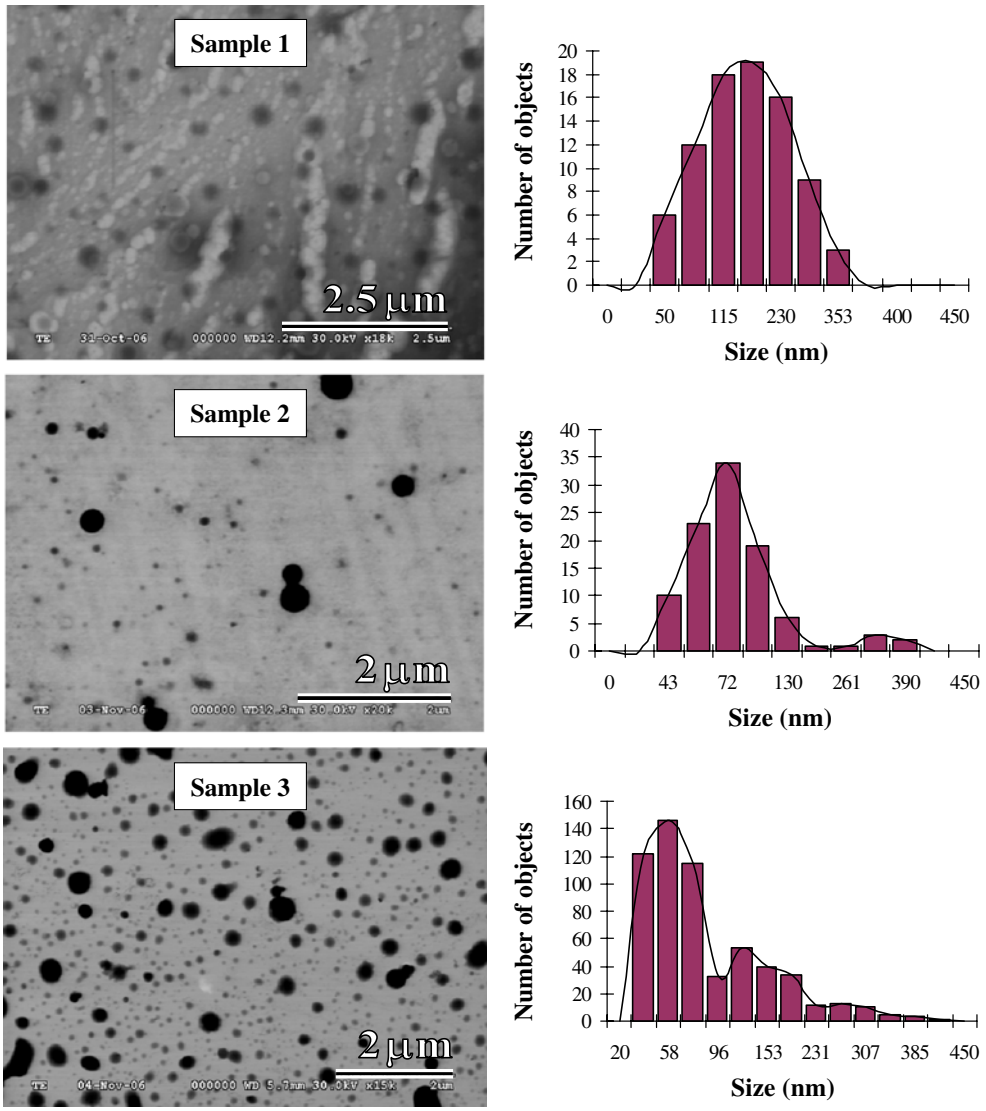

Fig. 6 TEM images and size distributions of low (sample 1), medium (sample 2), and high molecular weight (sample 3) ST/EGDM copolymer nanoparticles. Bar, 2.5 µm (sample 1), 2 µm (samples 2 and 3)

produced polymer chains have reacted. It is assumed that in that early stage of polymerization (t_r=30 min, conversion=9.4%), the quantity of pendant groups primarily participating in additive reactions when monomers M_1 and M_2 and macroradicals are added to the chains to form a highly branched polymer structure is predominant. Contrary to our expectations, particle size of solid sample was higher (180 nm) than the hydrodynamic diameter (12 nm; see Fig. 5 for sample 1) measured in the same polymer solution, and the difference is significant. In our view, the difference first is caused by the drying of the TEM sample, where the polymer originally globular morphology in solvent will unroll and becomes flatten to the extent of branched structure. The other reason is the DLS measurement, since low quantity of methanol was introduced to the sample solution in order to make the fully transparent polymer solution detectable. Additionally, the linear and the branched polymer samples have poor scattering properties during DLS measurement; thus, smaller apparent size was determined instead of the effective hydrodynamic diameter.

The distribution curve constructed on the basis of TEM images of sample 2 shows bimodal size distribution and higher polydispersity compared to sample 1. Particle sizes corresponding to the peaks in the distribution curve are 72 and 310 nm, which are 1.8 and 2.5 times larger than the hydrodynamic diameter measured in the solution by DLS (41 and 120 nm; see Fig. 5, sample 2). The above findings as well as the reduction of residual pendant vinyl groups (47.5%) make us assume that, in the course of the formation of sample 2, there are primary and secondary cyclization reactions in addition to the addition reactions typical of pendant groups. Such reactions form the so-called 'microgel' structure consisting of intramolecular crosslinks; the increased contrast in TEM picture also supports this hypothesis (Fig. 6).

In case of sample 3, the distribution curve constructed on the basis of TEM picture shows multimodal distribution and even higher polydispersity. Particle sizes corresponding to the peaks in the distribution curve are 58, 115, and 269 nm, which are quite close to the hydrodynamic diameters measured in the solution by DLS (see Fig. 5 and sample 3). The unreacted pendant vinyl group content calculated on the basis of NMR spectrum is as low as 16.3%. Prolonged reaction time and high initiator concentration make it possible that the overwhelming part of pendant vinyl groups of EGDM units in the polymer react. Consequently, polymer nanoparticles have highly crosslinked structure. The particle size in solid state correlates well with the diameters measured in the solution by DLS (59, 163, and 324 nm), which also indicates that having such crosslinked structure prevents the formation of 'flattened' shape and intensive swelling as well.

Since TEM analysis provides only limited information on the morphology of polymer particles, SEM studies were also introduced. The results of SEM analyses are illustrated in Fig. 7. The studies showed that polymer samples 1 and 2 consist of particles of generally regular circular cross-section different in size, whereas sample 3 also have irregular and prolate polymer samples similar to strawberry (see Fig. 7a–c). At the same time, the image taken of sample 1 is less contrastive, which is typical of the highly flattened (non-circular in cross-section) shapes of the polymer particles. The non-crosslinked structure promotes the formation of such flattened shape (higher apparent size). Molecular weight of sample 2 is higher and has partly crosslinked structure; SEM picture of this sample is contrast and shows higher polydispersity. The SEM image taken of sample 3 is not typical of the entire polymer sample (primarily consists of particles of spherical symmetry) but deemed important to present in order to understand clearly the sub-processes taking place during synthesis. Large and asymmetric particles appear because long reaction times and high initiator concentration allow interparticular reactions to take place among reactive, highly branched polymer 'microgels' of partly crosslinked structure formed in different molecular weights during propagation. Such large and irregular polymer particles cannot be seen in TEM pictures, for they tend to adhere to the coal layer above the copper grid. Figure 8 shows the possibility of formation of asymmetric polymer nanoparticles.

Figure 7d–f allows a conclusion on the film-forming abilities of the polymers studied. Higher polymer concentration (1 mg/ml) was applied to make samples, and certainly, no tenside was added at all, not even to polymer samples of low molecular weight. It can be seen that sample 1 forms a complete film with soft contours where the estimated thickness is about 80 nm. Sample 2 is also able to form complete film (although with more indented contour), whereas no complete film can be made from sample 3 under identical conditions. The differences in film-forming abilities of the analyzed samples can also be attributed to the differences in molecular weights and crosslink densities of the polymers.

Conclusions

Polymeric particles were synthesized by free radical nonlinear copolymerization of ST and EGDM. Crosslinking reactions were performed up to the gelation point. Low molecular weight, perfectly soluble branching polymers, medium molecular weight, soluble/swelling microgels, or very high molecular weight, and swelling/particularly soluble, forming stable colloid solution polymer particles

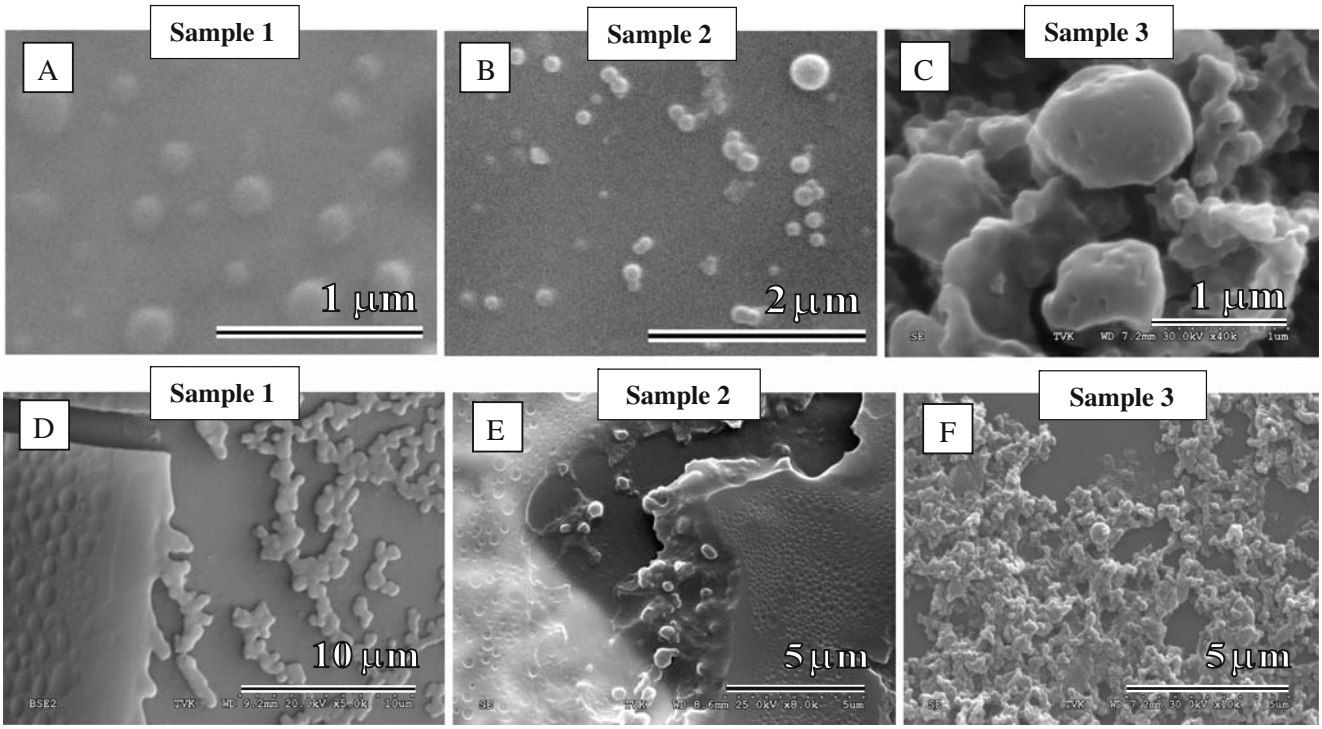

Fig. 7 SEM images of low (sample 1), medium (sample 2), and high molecular weight (sample 3) ST/EGDM copolymer nanoparticles. **a**–**c** Morphology of the low, medium, and high molecular weight ST/EGDM polymer nanoparticles. Bar, 1 μm (samples 1 and 3), 2 μm (sample 2). **d**–**f** Film formation of low, medium, and high molecular weight polymer samples. Bar, 10 μm (sample 1), 5 μm (samples 2 and 3)

were obtained depending on the initiator concentration and total concentration of the monomer and the crosslinker.

There are three conclusions to draw from this study. (1) A synthesis method has been developed, in which polymer nanoparticles can be produced at very high conversion rate by applying solution, radical polymerization at high crosslinkage rate (monomer feed, ST/EGDM=1/1). Nearly 100% conversion was observed at 0.278 mol/dm^3 monomer concentration and at 20 mol% AIBN. The synthesized polymer is highly branched and has partially crosslinked structure, of which stable colloid solution can be produced. (2) By analyzing samples with low, medium, and high molecular weights (GPC, DLS, TEM, and SEM) the subprocesses taking place in the course of syntheses was studied. It was established that polymer with low molecular weight is highly branched in structure, which is produced through addition reactions of monomers and macroradicals with pendant double bonds on primary chains. Since in the course of formation of samples with medium and high molecular weights, intraparticular cyclization reactions also take place, those materials already have crosslinked structure in parts. In addition, as the result of interparticular

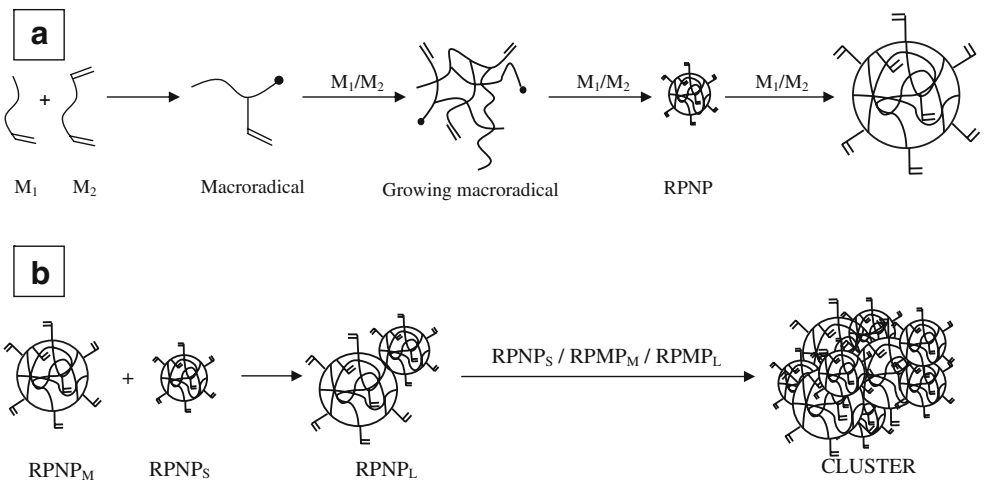

Fig. 8 Schematic illustration of the formation of symmetrical (**a**) and asymmetrical (**b**) polymer nanoparticles (*RPNP* reactive polymer nanoparticles, *S* small, *M* medium, *L* large)

reactions, asymmetric particles also appeared in the polymer sample with large molecular weight (3). It was established that, by controlling polymerization subprocesses through changing reaction conditions ([mon], [I], t_r) (without changing monomer composition), the structure and morphology of polymer materials [hence, the macroscopic characteristics (film formation)] can be influenced purposely.

Acknowledgment The work was supported by RET (Grant of Regional University Knowledge Center) contract number (RET-06/423/2004) and in part by ElizaNor Polymers LLC, New Jersey, USA. The authors would like to thank Zsolt Dudas for taking the SEM micrographs (Tisza Plastic Company).

References

1. Voit BJ (2000) Polym Sci, Part A: Polym Chem 38:2505–2525
2. Seiler M (2002) Chem Eng Technol 25:237–253
3. Kharchenko SB, Kannan RM, Cernohous JJ, Venkataramani S (2003) Macromolecules 36:399–406
4. Kharchenko SB, Kannan RM (2003) Macromolecules 36:407–415
5. Furukawa T, Ishizu K (2003) Macromolecules 36:434–439
6. Gao C, Yan D (2004) Prog Polym Sci 29:183–275
7. Peppas NA, Nagai T, Miyajima M (1994) Pharm Tech Jpn 10:611
8. Widawski G, Raviso M, Francois B (1994) Nature 369:387–389
9. Szaloki M, Bukovinszki K, Uveges A, Hegedus C, Borbely J (2007) Fogorvosi Szemle 100(6):307–312, (in Hungarian)
10. Borbely J, Uveges A, Szatmari M (2003) US Patent Application 11/414953
11. Flory PJ (1941) J Am Chem Soc 63(11):3083–3100
12. Deng H, Kanaoka S, Sawamoto M, Higashimura T (1996) Macromolecules 29:1772–1777
13. Kanaoka S, Hayase N, Higashimura T (2000) Polym Bull 44:485–492
14. Okay O, Funke W (1990) Makromol Chem Rapid Commun 11:583–587
15. Abrol S, Solomon DH (1999) Polymer 40:6583–6589
16. Gurr PA, Qiao GG, Solomon DH, Harton SE, Spontak RJ (2003) Macromolecules 36:5650–5654
17. Zhang X, Xia J, Matyjaszewski K (2000) Macromolecules 33:2340–2345
18. Sawamoto M, Kamigaito M (2001) Polym Mater Sci Eng 84:361
19. Baek K-Y, Kamigaito M, Sawamoto M (2002) Macromolecules 35:1493–1498
20. Lord HT, Quinn JF, Angus SD, Whittaker MR, Stenzel MH, Davis TP (2003) J Mater Chem 13:2819–2824
21. O'Brien N, McKee A, Sherrington DC, Slark AT, Titterton A (2000) Polymer 41:6027–6031
22. Costello PA, Martin IK, Slark AT, Sherrington DC, Titterton A (2002) Polymer 43:245–254
23. Isaure F, Cormack PAG, Sherrington DC (2003) J Mater Chem 13:2701–2710
24. Slark AT, Sherrington DC, Titterton A, Martin IK (2003) J Mater Chem 13:2711–2720
25. Isaure F, Cormack PAG, Sherrinhton DC (2004) Macromolecules 37:2096–2105
26. Bütün V, Bannister I, Billingham NC, Sherrington DC, Armes SP (2005) Macromolecules 38:4977–4982
27. Li Y, Armes SP (2005) Macromolecules 38:5002–5009, 8155–8162
28. Bannister I, Billingham NC, Armes SP, Rannard SP, Findlay P (2006) Macromolecules 39:7483–7492
29. Vo C-D, Rosselgong J, Armes SP (2007) Macromolecules 40:7119–7125
30. Wang AR, Zhu S (2005) Polym Eng Sci 45:720–727
31. Wang AR, Zhu S (2005) J Polym Sci 43:5710–5714
32. Sato T, Hashimoto M, Seno M, Hirano T (2004) Eur Polym J 40:273–282
33. Hirano T, Tanaka K, Wang H, Seno M, Sato T (2005) Polymer 46:8964–8972
34. Hirano T, Ihara H, Miyagi T, Wang H, Seno M, Sato T (2005) Macromol Chem Phys 206:860–868
35. Ho AK, Lin L, Gurr PA, Mills MF, Qiao GG (2005) Polymer 46:6727–6735
36. Uveges A, Szaloki M, Hartmann JF, Hegedus C, Borbely J (2008) Macromolecules 41:1223–1228
37. Szuromi M, Merka M, Borbely J (2000) Macromolecules 33:3993–3998